J Therm Spray Tech (2024) 33:619–628
https://doi.org/10.1007/s11666-024-01752-0

ORIGINAL RESEARCH ARTICLE

Mixed-Material Feedstocks for Cold Spray Additive Manufacturing of Metal–Polymer Composites

Matthew S. Schwenger[1] · Madison S. Kaminskyj[1] · Francis M. Haas[1] · Joseph F. Stanzione III[1]

Submitted: 16 June 2023 / in revised form: 10 February 2024 / Accepted: 17 February 2024 / Published online: 15 March 2024

Abstract High-performance polymers such as poly(ether ether ketone) (PEEK) are appealing as composite components for a wide variety of industrial and medical applications due to their excellent thermomechanical properties. However, conventional PEEK metallization methods can often lead to poor quality control, low deposition rate, and high cost. Cold spray is a promising potential alternative to produce polymer–metal composites rapidly and inexpensively due to its relatively mild operating conditions and high throughput. In this study, we investigated the deposition characteristics of metal–polymer composite feedstock, composed of PEEK powder and copper flake in varying ratios, onto a PEEK substrate. Copper-PEEK powder blends were prepared by both hand-mixing and cryogenic milling (cryomilling), which predominantly creates composite particles with micron-scale copper domains coating PEEK particle surfaces. This process non-monotonically affects the relative dominance and length scales of the multiple contributing deposition mechanisms present in mixed-material cold spray. In low-pressure cold spray, deposits showed significant changes in deposition efficiency and composition as a result of milling, with improvements in these characteristics most dramatic at lower Cu fractions. Deposits of a cryomilled blend of nominally 30 vol.% copper in PEEK exhibited minimal porosity under scanning electron microscopy, complete retention of powder composition, and the highest deposition efficiency among all samples tested. Notably, neither neat PEEK nor neat Cu meaningfully deposited at the same mild conditions as this 30 vol.% Cu blend, indicating a synergistic departure from linear mixing rules driven by the relative balance of local deposition interactions (e.g., hard–soft, soft–soft, etc.). Intentional powder and process design toward optimizing this balance may facilitate cold spray metallization applications.

Keywords bond layer · cold spray · composite feedstock · cryogenic milling · metallization · poly(ether-ether-ketone) · powder preparation

Matthew S. Schwenger and Madison S. Kaminskyj have contributed equally to this work.

This article is an invited paper selected from presentations at the 2023 International Thermal Spray Conference, held May 22–25, 2023, in Québec City, Canada, and has been expanded from the original presentation. The issue was organized by Giovanni Bolelli, University of Modena and Reggio Emilia (Lead Editor); Emine Bakan, Forschungszentrum Jülich GmbH; Partha Pratim Bandyopadhyay, Indian Institute of Technology, Karaghpur; Šárka Houdková, University of West Bohemia; Yuji Ichikawa, Tohoku University; Heli Koivuluoto, Tampere University; Yuk-Chiu Lau, General Electric Power (Retired); Hua Li, Ningbo Institute of Materials Technology and Engineering, CAS; Dheepa Srinivasan, Pratt & Whitney; and Filofteia-Laura Toma, Fraunhofer Institute for Material and Beam Technology.

✉ Matthew S. Schwenger
schwengem5@rowan.edu

[1] Advanced Materials and Manufacturing Institute, Rowan University, Glassboro, NJ, USA

Introduction

In the metallization of polymers by cold spray, most work to date has focused on spraying metal particles directly onto polymer and fiber-reinforced polymer substrates (Ref 1). One common metal–polymer combination for metallization is Cu and PEEK, which is heavily utilized in the aerospace industry (Ref 2). PEEK matrix-composite aircraft structures have a high specific electrical resistivity

and are therefore prone to lightning strikes (Ref 3). As a result, Cu coatings on such polymer-rich composites provide improved electrical conductivity and electromagnetic interference (EMI) shielding to the aircraft (Ref 2). In studies of metallization by cold spray, nominal processing temperatures and pressures often range from 150 to 600 °C and 0.5-5 MPa, depending on the substrate and sprayed material. In Cu-PEEK systems specifically, operating temperatures and pressures largely exceed 300 °C and 1.5 MPa, but the resulting metallic coatings were reported to have less than desirable properties both in mixed-material cold spray (Ref 4, 5) and direct metallization (Ref 6). One reason for poor properties at the Cu-PEEK interface in direct metallization is the interfacial porosity induced by the cold spray process (Ref 6). Due to the difference in hardness between the Cu particle and PEEK substrate, cold-sprayed Cu embeds in the PEEK substrate and deposits by mechanical interlocking rather than undergoing plastic deformation and jetting due to adiabatic shear. Furthermore, when PEEK and Cu were sprayed in tandem, the compositions of the final deposits were more polymer-rich than the original feedstocks (Ref 4, 5), most notably at lower pressures (Ref 5), indicating a preferential deposition of PEEK over Cu during spray.

When cold spraying two materials in tandem, multiple deposition mechanisms must be considered, which can be related to the relative hardness of the spray media. When a particle of the softer material (i.e., PEEK) impacts a region of the harder material (i.e., Cu) or vice versa, only the soft material undergoes plastic deformation (Ref 7). Effectively, a soft particle splatters on a hard substrate (soft/hard interaction), and a hard particle becomes embedded in a soft substrate (hard/soft interaction). In impacts of a hard or soft particle on the same material, the extent of plastic deformation in both the particle and substrate is still dependent on the mechanical and interfacial properties of the material. Notably, when PEEK and Cu were sprayed simultaneously on PEEK substrates, impinging Cu particles were only observed to deform upon impact with embedded Cu when no oxide layer was present at either surface (Ref 4). In the same study, Cu comprised 80 vol.% of the total feedstock and therefore the hard/hard interaction was overwhelmingly dominant in these experiments. However, because only PEEK underwent visible plastic deformation during cold spray, very few contact points between Cu particles existed, leading to electrical conductivity measurements two orders of magnitude lower than that of bulk Cu.

Our approach to the metallization of PEEK is to alter the deposition mechanism of the spray and thereby minimize the porosity formed at the Cu-PEEK interface. To accomplish this, we fabricated Cu-PEEK composite particles by cryogenic milling. High-energy ball milling has been previously shown to fabricate Cu-W composite particles with micron-scale domains (Ref 8), but cryogenic milling was reported to achieve more uniform particle dispersion in a polymer-ceramic system of ethylene–vinyl acetate copolymer and barium titanate (Ref 9). In the Cu-W study, high-energy ball milling was used as an alternative to spraying Cu and W particles simultaneously because of the poor adhesion properties observed in the W particles. Incorporating the two materials into a composite feedstock improved both the overall deposition efficiency of the process and the W content of the final deposit. Larger grains and lower overall concentrations of W both correlated to higher deposition efficiency (DE) in milled Cu-W composite cold spray (Ref 8). In consideration of these findings, we dispersed microscopic Cu domains throughout the PEEK particles by cryogenic milling. In this study, multiple Cu-PEEK composite powders were prepared by hand-mixing and cryogenic milling and deposited via low-pressure cold spray. The DE, porosity, hardness, and Cu content by weight were measured for each deposit, and co-deposition methods of Cu and PEEK powder blends under mild processing conditions were observed. The threshold of Cu concentration in the initial powder blends for successful deposition and lower porosity was determined.

Experimental Methods

Materials and Sample Preparation

Poly(ether ether ketone) (PEEK) powder with a nominal particle size of 50 µm was acquired from Goodfellow, USA. Copper flake (>99% purity) with a nominal size of 325 mesh (44 µm) was acquired from Alfa Aesar. All powder samples were prepared gravimetrically and hand-mixed to achieve target nominal volume fractions defined by the true densities of PEEK and copper. The various nominal volume fractions of Cu indicated in Table 1 were selected to create significant variation in both Cu concentration and domain size across the population of tested feedstocks while keeping the overall mass content of all samples predominantly Cu-based for potential applications in EMI shielding. PEEK substrates of thickness 3.175 mm (0.125”) were cut to 75 × 75 mm squares using a table saw with no additional surface preparation.

Cryogenically ball-milled (cryomilled) composite powders were prepared in a Retsch Cryomill using a 50-mL vessel loaded with a 25-mm stainless steel ball. Approximately 15-20 cm^3 of hand-mixed powder was added to the vessel in each batch, which was processed in six milling cycles after one minute of initial cooling. Each milling cycle consisted of five minutes of grinding at an oscillation rate of 30 Hz, followed by one minute of post-grind

Table 1 Nominal volume fractions of Cu-PEEK blends and corresponding mass fractions

Nominal Cu volume, vol.%	Cu content, wt.%	Cu content by TGA, wt.%
20	63.1	66.7 ± 2.4
30	74.6	74.2 ± 0.7
40	82	84.2 ± 0.9
50	87.2	86.5 ± 0.03
60	91.1	91.9 ± 0.4

cooling. The cryomilled powders were passed through a No. 70 mesh sieve to promote flowability and separate agglomerates that formed during the milling process.

All powder blends and composite powders described in this study are labeled by their composition and method of preparation using an XXXX-Y format, where XXXX indicates the volume percent of each component in the mixture (e.g., 2080 designates mixtures composed of 20 vol.% Cu, 80 vol.% PEEK) and Y indicates whether the sample is a hand-mixed (H) or cryomilled composite (C) feedstock. No sieving was required for the H feedstock as it was not subject to any processing that would reduce flowability or create agglomerates.

To determine suitable cold spray operating conditions for the H and C feedstocks, neat PEEK powder was analyzed using differential scanning calorimetry (DSC) with a TA Instruments DSC2500. In polymer cold spray, previous work has indicated that the carrier gas temperature should be between the glass transition temperature, T_g, and melt temperature, T_m, of the polymer (Ref 10-12). When heated at a rate of 10 K min^{-1}, PEEK was found to have a T_g of 149.8 ± 0.3 °C and a T_m of 343.7 ± 0.2 °C.

Low-Pressure Cold Spray and Macroscopic Analyses

The low-pressure cold spray apparatus, CSM 108, was acquired from Gold Plating LTD. The apparatus was modified to utilize an ambient downstream rotary drum powder feeder that helps deposit powder in a continuous flow at a controlled rate (Ref 11). The CSM-108 nozzle measurements are length 138 mm, throat diameter 2.52 mm, exit inner diameter 10.8 mm, and is further described in Ref 13. A suction line runs from the feeder to the spray nozzle, where powder is then accelerated by pre-heated gas (Ref 11). The choice of suitable operating parameters was informed by the temperature-dependent behaviors of PEEK observed through DSC, as well as upper temperature limits of the cold spray apparatus. The operating parameters for cold spray remained constant for each volume ratio and each feedstock type (Table 1), neat PEEK, and neat Cu. Using air as the carrier gas, each sample was sprayed at a nominal gas temperature of 200 °C and nominal pressure of 8 bar with a fixed 20 mm initial standoff distance. Though the rotation rate of the rotary drum powder feeder was also kept constant, feed rates varied between the cryomilled and hand-mixed powder blends due to significant bulk density variation among feedstocks. The spray path of rectangular coupons also remained constant, and each volume ratio and feedstock type were sprayed in triplicate to determine deposition efficiency (DE). The spray path consisted of a 4-pass,10-line spray path with a length of 60 mm, a step size of 2 mm, and had a nozzle raster speed of 1000 mm*min^{-1}. DE was determined by the ratio of the weight of the deposited powder to the weight of the powder sprayed. The hardness of the deposits was measured five times per sample on a Shore D durometer from PTC Instruments.

Composition Measurements by Thermogravimetric Analysis (TGA)

Samples of cold-sprayed deposits weighing 8-10 mg were removed from PEEK substrates and heated to 900 °C in air using a TA Instruments TGA550 thermogravimetric analyzer operated at a heating rate of 10 K min^{-1}. The composition of each deposit and feedstock was determined by the mass balance:

$$x_{Cu} = \frac{m_{f,\,dep} - m_{f,\,PEEK} x_{PEEK}}{m_{f,\,Cu}} \quad \text{(Eq 1)}$$

where $m_{f,i}$ is the remaining mass of each material i at 900 °C and x_i is the mass fraction of each component present in the deposit. This model assumes that no reaction occurs between the Cu and PEEK that would impact the final char yield of either species. To ensure that deposits with higher Cu content achieved full oxidation, a two-hour isothermal dwell at 900 °C was employed for 3070, 4060, and 5050 blends, and a four-hour dwell at 900 °C was employed for 6040 blends.

Microscopy of Powders and Deposits

Hand-mixed powder blends, cryomilled composite powders, and cold spray deposit surfaces and cross sections were examined using a Phenom XL scanning electron microscope (SEM). For the cold spray deposit microstructures, a small segment of the deposit was

stripped from the substrate with a razor blade, which could have caused slight damage or void spaces to the deposit. Images of the deposit microstructures were taken at an accelerating voltage of 5 kV and chamber pressure of 60 Pa.

Results and Discussion

Feedstock Characterization

As shown in Fig. 1, neat PEEK powder was found to retain no mass after decomposition in air, and the mass of Cu was found to increase by 25 wt.%, indicating complete oxidation to CuO. Based on these results, Eq 1 can be simplified to the following expression:

$$x_{\mathrm{Cu}} = \frac{m_{f,\,\mathrm{dep}}}{1.25} \qquad \text{(Eq 2)}$$

Shown in Fig. 1 are the TGA thermograms of the 3070-H and 5050-H feedstock powders, which exhibit identical behavior to the pure Cu flake until mass loss begins at $\sim$ 350 °C. While the presence of Cu appears to induce the decomposition of PEEK at much lower temperatures than observed in the neat polymer powder, this effect has minimal impact on the final char yield of each mixture. Applying Eq 2, we calculate Cu contents of 74.2 $\pm$ 0.7 wt.% and 86.4 $\pm$ 0.03 wt.% for the 3070-H and 5050-H powders, respectively, closely matching weight ratios described in Table 1 and confirming the assumption made in Eq 1. Since no mass is gained or lost in the cryomilling process, it is reasonable to assume that the Cu content in the 3070-C and 5050-C powders are identical to the corresponding H powders.

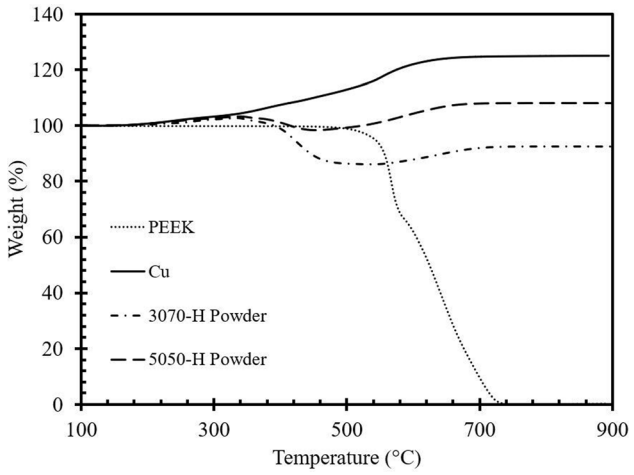

Fig. 1 Thermogravimetric analysis (TGA) of neat PEEK, Cu, 3070-H, and 5050-H powders

Both hand-mixed and cryomilled powders are shown in Fig. 2, where Cu and PEEK are indicated by light and dark regions, respectively. Figure 2(b)–(f) shows that cryomilled samples in each volume ratio except 6040-C generate Cu particles with few small PEEK domains, PEEK-rich particles with micron-scale Cu domains, and < 20 µm Cu particles with no visible regions of PEEK. Blends with lower Cu content appear to generate larger PEEK-rich particles while the blends with higher Cu content consist largely of Cu-rich and pure Cu particles. This is likely due to the additional compressive forces imposed on the PEEK particles by the increased Cu particle concentration during cryomilling. These compressive forces also serve to either consolidate or shatter the porous and dendritic particles within the Cu flake, which can be seen in Fig. 2(a). Very few Cu particles in Fig. 2(b), (c), and (d) appear to be dendritic in shape or have much visible porosity, implying that the dendritic components of the Cu flake either shatter and incorporate into the PEEK particles during cryomilling or are compressed and consolidated by or into neighboring Cu particles. As the Cu content increases, two trends arise: solid Cu particles become more prevalent, and PEEK particles appear to have fewer micron-scale Cu domains on their surfaces, indicating a preference for consolidation over shattering as the Cu fraction increases. One potential explanation for this is that when a porous or dendritic particle breaks during cryogenic milling, the small Cu fragments are more likely to collide with and adhere to other Cu particles as the volume fraction of PEEK decreases.

Cold Spray Deposit Characterization

In a previous work, both multi-pass and single-pass deposition efficiencies were compared for Cu-PEEK mixtures and composite powders (Ref 14). The absence of significant difference in single-pass deposition efficiency implied a strong similarity in the particle-substrate interactions with each Cu-PEEK feedstock, regardless of Cu content or preparation. Thus, this study focuses on the deposits formed by multiple passes to develop a more robust understanding of the inter-particle interactions within the feedstock powder.

As shown in Fig. 3, not only is DE a function of the Cu content of the feedstock powder, the extent to which cryomilling the feed improves DE also shifts with feed composition. At lower Cu fractions, the effect of cryomilling is most pronounced, increasing from 23.3 to 36.1% in the 2080 powders and from 31.5 to 41.6% in the 3070 blends. As the Cu content increases further, the gap between the H and C DE values monotonically decreases to the point where no benefit can be observed in the case of the 6040 samples. This trend is most likely due to the increasing

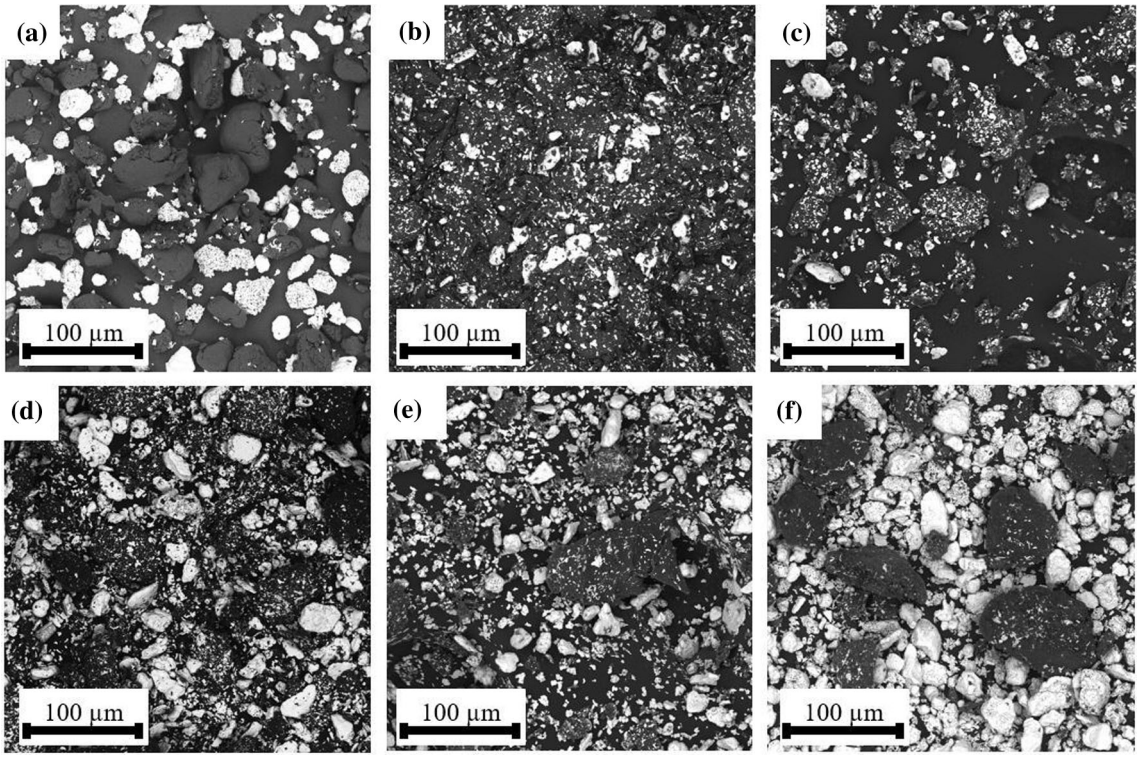

Fig. 2 SEM micrographs of (a) 2080-H, (b) 2080-C, (c) 3070-C, (d) 4060-C, (e) 5050-C, and (f) 6040-C powder blends

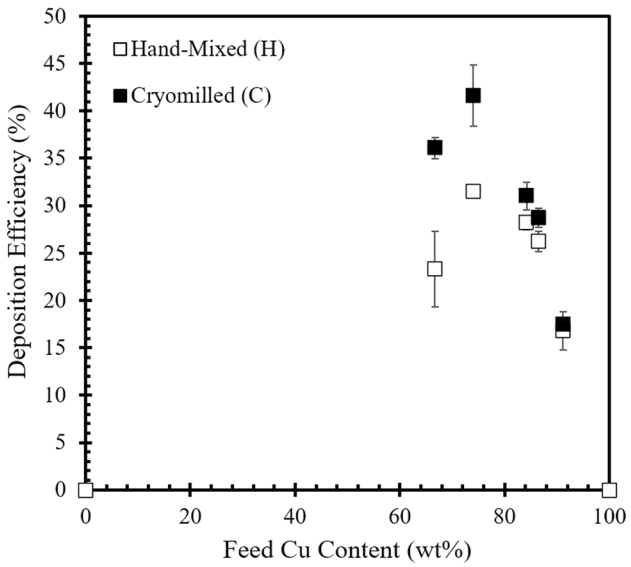

Fig. 3 Deposition efficiency (DE) of Cu, PEEK, and their composite blends

concentration of dense Cu particles still present in the cryomilled blends with increasing Cu fraction. Because the powder blends are sprayed at a gas temperature and pressure of 200 °C and 8 bar, greater presence of Cu particles past 75 wt.% (3070 blends) only serves to reduce DE as copper cannot deposit on itself or onto neat PEEK at such mild conditions. Using air as a carrier gas may also create a small oxide layer on the Cu particles, creating yet another barrier to deposition. Comparing the feed powders shown in Fig. 2, the increased prevalence of Cu-rich and pure Cu particles in the cryomilled mixtures with higher Cu content implies a greater influence of hard–soft and hard–hard interactions on the overall deposit quality.

In the composition analysis shown in Fig. 4(a), deposits of the cryomilled feed powder showed improved composition retention over the corresponding hand-mixed powder in the case of the 2080 blends. As the Cu content in the C samples increased, however, the final Cu content of the deposit deviated farther from the initial composition of the feed. The H samples showed a more consistent linear trend in Cu content after deposition, but largely demonstrated preferential deposition of PEEK, similar to previous observations (Ref 4, 5). As noted in Ref 5, Cu content in the deposit decreases as carrier gas pressure decreases since the resulting velocity of the Cu particle is insufficient for successful embedding on the PEEK substrate or deposition onto previously bonded Cu particles. Similar behavior was observed in the C powders at high Cu fractions, indicating a reduction in the effect of cryomilling as dense Cu particles become increasingly prevalent in these feed blends. Conversely, as seen in Fig. 4(b), the hardness of each deposit appears to be an essentially linear function

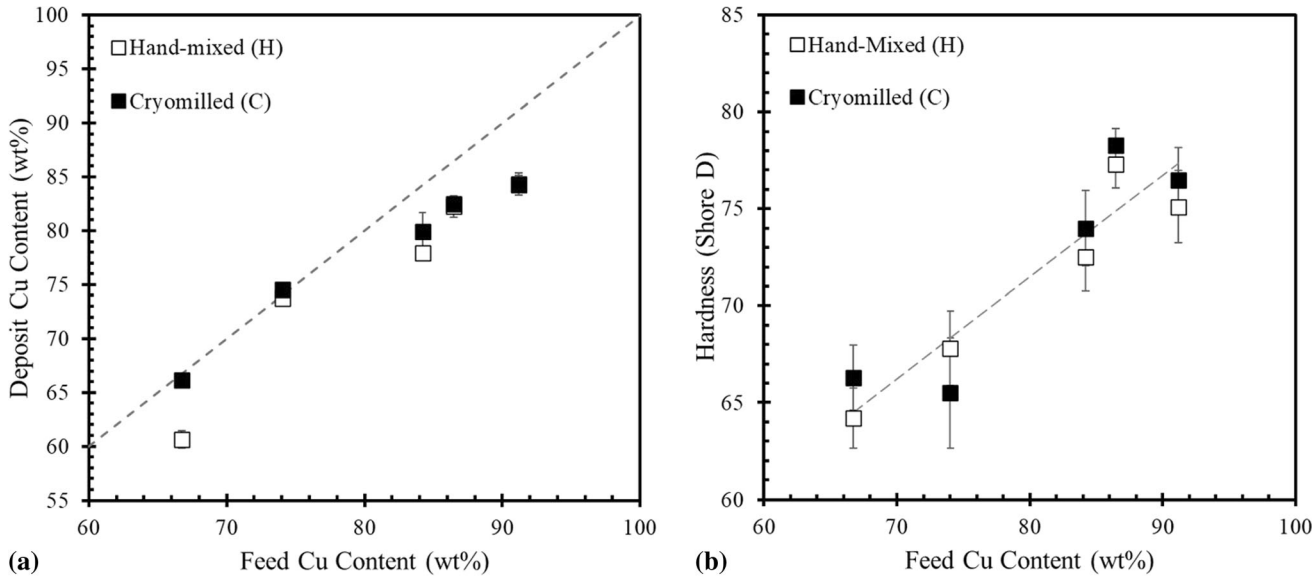

Fig. 4 (a) Cu content and (b) shore D hardness of cold-sprayed deposits of Cu-PEEK blends

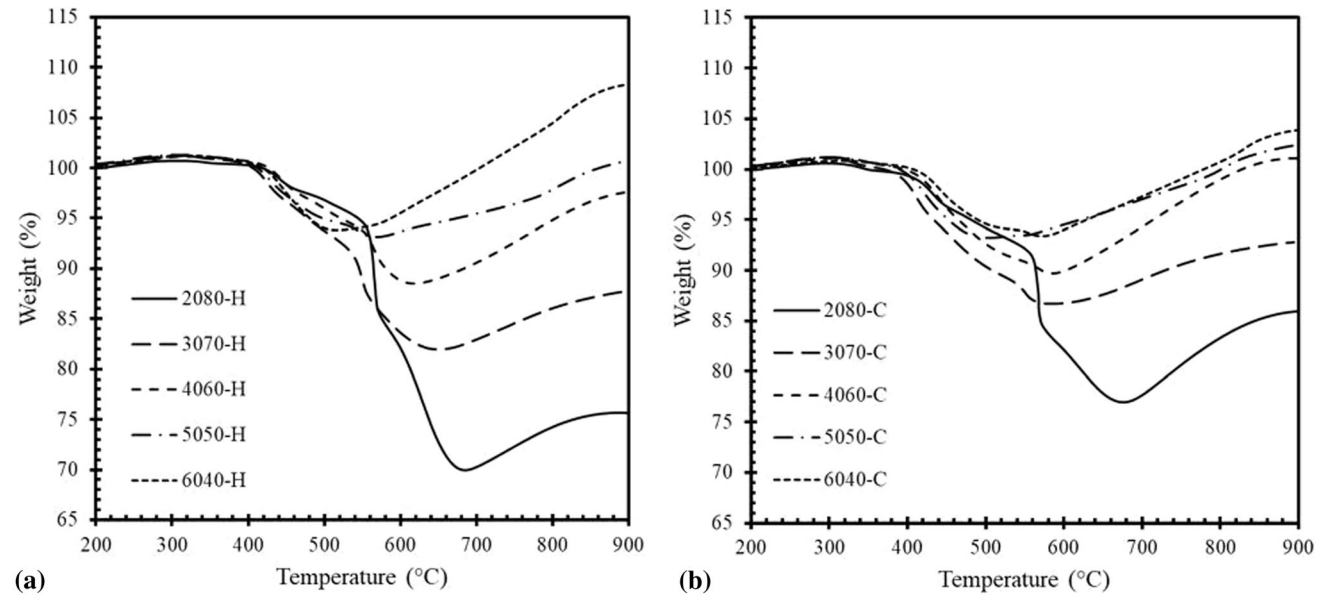

Fig. 5 Thermograms of cold-sprayed deposits of (a) hand-mixed and (b) cryomilled powder blends

of the Cu content of the feedstock, indicating no effect of cryomilling on deposit hardness.

Unlike the TGA of the precursor powders shown in Fig. 1, thermograms of the cold-sprayed composites in Fig. 5 appear to undergo a complex multi-stage decomposition and oxidation. The characteristic mass gains associated with the oxidation of the Cu component are delayed in their onset and appear to occur over a longer temperature range. The decomposition of PEEK in each sample shows similarly slowed onset rates and overall time frames when compared to the 3070-H and 5050-H powders analyzed in Fig. 1, suggesting that these changes in decomposition behavior are due to limited mass transfer through the deposit samples during TGA. Since mass transfer limitations only affect the rate at which mass change occurs and not the underlying reactions, Eq 2 can still be used to compute the Cu content of cold-sprayed deposits.

With careful consideration, the onset temperature and initial rate of mass loss may provide insight into the microstructure of deposits without analysis by SEM. As seen in Fig. 1, the onset of mass loss occurred in the Cu-

PEEK powder mixtures roughly 200 K sooner than in neat PEEK. However, much greater variety can be seen between the cold spray deposit thermograms. Not only do the low Cu-content H and C deposits reach different minimum weight fractions, further reiterating the lower Cu fraction in the H samples presented in Fig. 4(a), but the onset of mass loss occurs earlier in these C samples compared to their H counterparts. Because the pure Cu curve shows that Cu only gains mass during the oxidative TGA, we can conclude any mass loss observed is due to decomposition of PEEK, in which case an earlier onset of decomposition indicates either an apparent catalytic effect of Cu on the PEEK particles or a mass transfer and reaction rate effect due to particle morphology changes during milling. Thus, deposits with higher Cu-PEEK interfacial area would exhibit a faster apparent reaction onset temperature and initial rate, as is observed in Fig. 5.

As shown in Fig. 2, cryogenic milling creates fine domains of Cu on PEEK particles and vice versa. The cryomilled samples, therefore, generally tend to exhibit earlier and more rapid mass loss due to the presence of these composite particles with high Cu-PEEK interfacial areas. Conversely, the deposits from hand-mixed powder blends tend to show a later onset of mass loss because the Cu-PEEK interfaces only occur at the boundaries of well-adhered particles. This effect is most prevalent in the 3070 samples, implying that this is the composition where cryomilling has the strongest effect on deposit microstructure.

While analysis of TGA provides some insight to the effects of cryomilling on microstructure, using TGA as a method of qualitatively understanding microstructure as a function of composition must be done much more carefully. As previously mentioned, the onset of decomposition observed in TGA is not a function directly of microstructure, but one of interfacial area. Thus, a deposit with a very low Cu fraction, such as the 2080 samples, will most likely have a lower Cu-PEEK interfacial area than one with a more balanced ratio of components simply due to the lower surface area of Cu available for contact with the predominantly PEEK matrix. Hence, when comparing the 2080-C TGA curve to those of the 4060-C and 5050-C deposits, one should note that the deposits have similar areas of intimate PEEK-Cu contact, but not similar microstructures. Due to the lower availability of Cu surfaces in 2080-C, the deposit microstructure is likely less porous than those of the 4060-C and 5050-C deposits.

Microstructural Observations

Cross sections of the deposits are presented in Fig. 6(a), in which the images were oriented such that the surface of the deposit was toward the top of each image. The most notable difference between the cryomilled and hand-mixed feedstock deposits is the improved consolidation in the cryomilled deposits, most notably at lower Cu fractions. While most of the C deposits still show some cracks originating at Cu-Cu and Cu-PEEK interfaces and propagating through the predominantly PEEK domain at low initial Cu fractions, the 3070-C deposit shows virtually no porosity or delamination except at the surface of the deposit. Further, in the 3070-C deposit, the Cu domains appear to be more deformed and in contact with one another than in the 4060-C sample despite having a lower Cu fraction. We believe this to be primarily due to the size, shape, and nature of the Cu domains in the 3070-C feedstock. The majority of the Cu in the 3070-C feedstock, as seen in Fig. 2(c), exists either as micron-scale or sub-micron domains surrounded by a PEEK matrix or as irregularly shaped particles with small PEEK domains incorporated therein, indicated by the small white areas on larger and otherwise darker particles. Consequently, hard/hard interactions during deposition occur almost exclusively at the surfaces of the Cu-PEEK composite particles and on a much smaller scale than conventional metallization methods. Rather, the soft/hard and soft/soft interactions of the Cu-reinforced PEEK particles appear to be the dominant deposition mechanisms in the 3070-C system. The smaller areas of hard/hard interaction also appear to encourage greater plastic deformation of Cu domains and particles, as evidenced by the horizontal shearing of Cu particles in the 3070-C deposit.

Below the nominal concentration of 30 vol.% Cu, there appears to be insufficient Cu present to exhibit the same effect upon deposition. While the 2080-C deposit appears to show more homogenous distribution of the micron-scale Cu domains seen in Fig. 2(b), cracking and delamination around Cu and Cu-rich particles are still present, which then propagate through larger PEEK domains as subsequent impacts occur. Looking at the 2080-C and 3070-C powders in Fig. 2, the feed blends appear to have similar distributions of Cu domains on the PEEK particle surfaces. Such similarity between the powders should result in analogous relative impacts of the various deposition mechanisms taking place, creating similar deposit microstructures. However, Fig. 6(a) shows that the reduced Cu fraction has a negative effect on deposit porosity. The higher concentration of dense Cu particles in the 3070-C powder may allow for a greater peening effect as deposition occurs. Thus, impacting and rebounding Cu particles may allow for greater deformation of deposited PEEK, penetrating into the cracks along sites of Cu deposition while the PEEK is still warm from the multiple passes of the gas jet.

Another effect of cryomilling on DE can be observed on the deposit surfaces. In Fig. 6(b), the surface of the 3070-H deposit appears to be populated with micron-scale strands

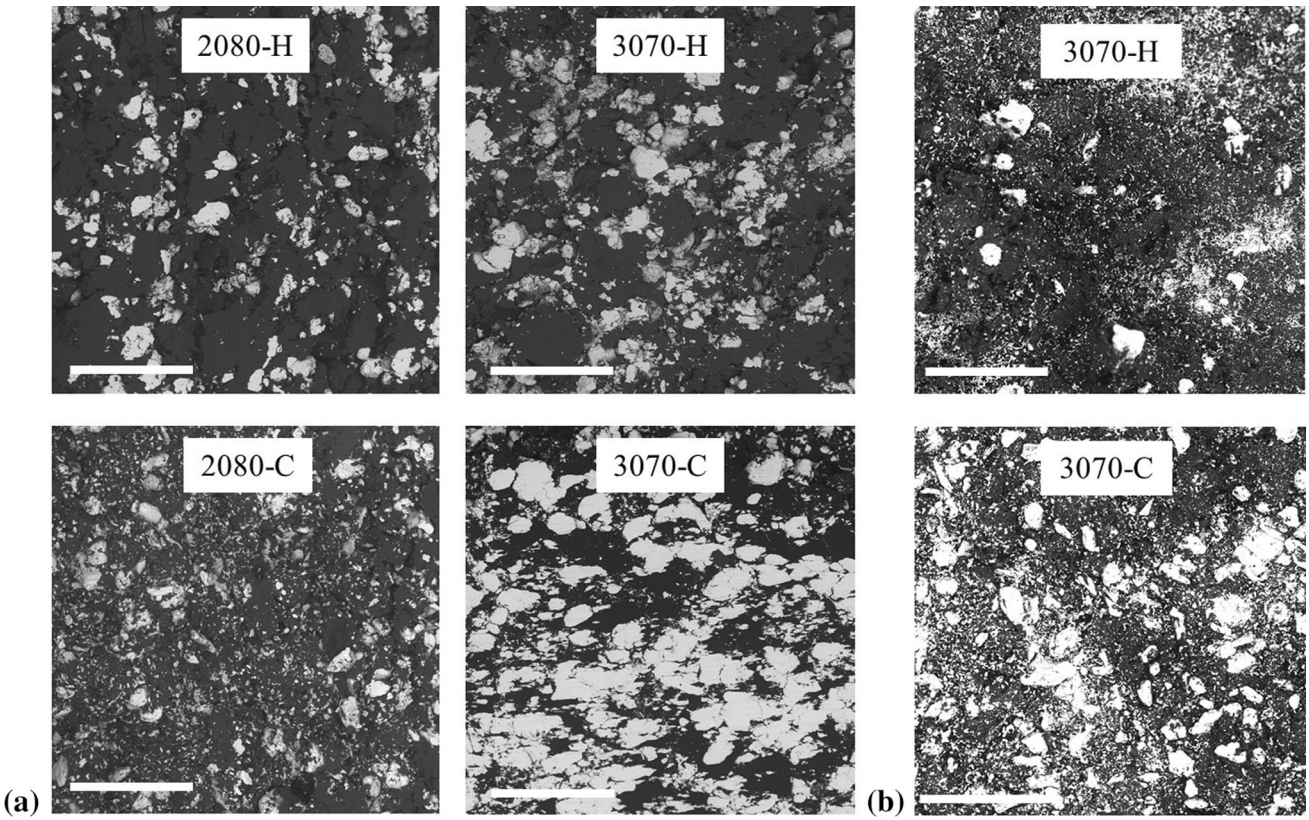

Fig. 6 SEM micrographs of (a) cross sections and (b) surfaces of 2080 and 3070 deposits. White, gray, and black domains correspond to Cu, PEEK, and voids, respectively

of Cu and few large Cu particles, despite the opposite being true in the hand-mixed powder blends as a whole (Fig. 2a). Because no porous or dendritic Cu particles are visible on the 3070-H surface, as were in the H feedstock mixtures, the light-colored strands and dots of Cu present on the surface SEM micrographs are the result of these more fragile particles shattering during cold spray. Whether these particles shattered on impact with the deposit or initially deposited and subsequently shattered as a result of impinging Cu particles from above is unclear. In the latter case, the energy absorbed by the shattering of the dendritic particles may cause the impinging Cu particle to rebound rather than deform and adhere, slightly reducing the overall Cu content in the final deposit. Conversely, these same dendritic particles are either compounded into the Cu-PEEK composite particles or into more dense Cu particles during cryomilling, which do not pose the same potential risk to deposition quality and may explain the apparently higher Cu content in the cross-section micrographs.

While increasing Cu content appears to provide some benefits via the peening effect, hard/hard interactions also become more prevalent, and mechanical deformation and interlocking are severely limited for Cu/Cu cold spray at the conditions used in this study. In the case of the 4060-C, 5050-C, and 6040-C deposits, shown in Fig. 7, the effect of this shift in deposition mechanism dominance can be seen most clearly at the boundaries of adjacent Cu particles, where minimal deformation occurs. In the corresponding H deposits, particle boundaries between adjacent PEEK particles are largely unclear, demonstrating effective deposition and cohesion by soft/soft interactions and compounding by subsequent Cu particle impacts. However, severe porosity and delamination primarily around Cu-Cu and Cu-PEEK boundaries indicate limited effectiveness in hard/soft and hard/hard interactions at the length scale of the sprayed particles. Although particle edges and boundaries at Cu-Cu impact sites are still well-defined in the 4060-C, 5050-C, and 6040-C cross sections, the reduction in porosity and separation at PEEK-Cu interfaces shows that cryomilling is still beneficial in feed powders whose deposition is dominated by hard-particle interactions.

Across the full range of Cu fractions tested, all except the 60:40 volume ratio show greatly improved deposit consolidation and fewer visible particle boundaries in the cryomilled blend deposits than in the analogous hand-mixed powders. The higher Cu fractions in these deposits, shown in Fig. 4(b), dictate that deposition mechanisms arising from hard-particle impacts will be the most prevalent during cold spray. However, in the cryomilled blends, more of the hard/hard and hard/soft interactions occur on a

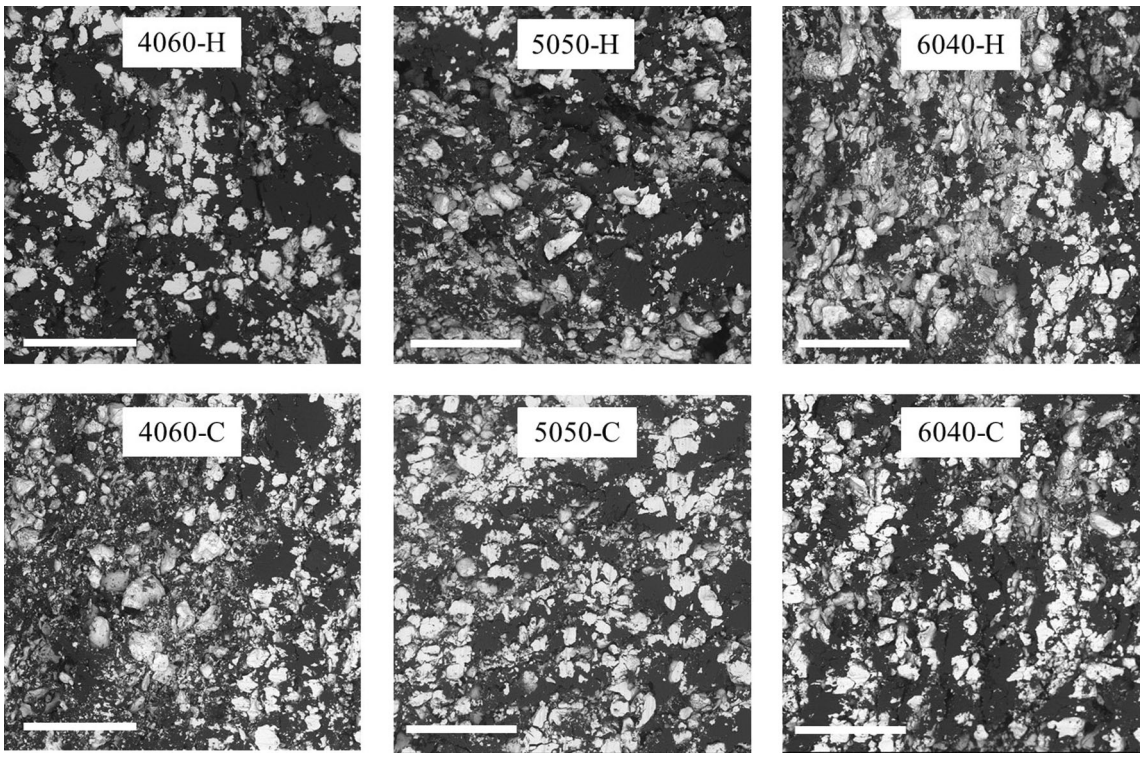

Fig. 7 SEM micrographs of 4060, 5050, and 6040 deposit cross sections. White, gray, and black domains correspond to Cu, PEEK, and voids, respectively

length scale more than an order of magnitude smaller than those in H feedstock blends due to the micron-scale Cu and PEEK domains on particle surfaces of the C powders. As seen in the 3070 deposits, shearing Cu is possible at these smaller length scales and impossible when only considering larger Cu particles. This shift in both relative dominance and nature of many deposition mechanisms not only visibly improves microstructure and deposit density, but significantly improves deposition efficiency, as shown in Fig. 3.

Conclusions

Overall, Cu and PEEK blends were shown to deposit on PEEK under relatively mild low-pressure cold spray conditions at much higher deposition efficiencies than either material sprayed alone. Across the compositions of powder blends tested, deposition efficiency was found to reach a maximum with nominal Cu volume fractions of 30%, correlating to 74.5% Cu by mass. At each composition, the cryomilled composite powders outperformed the hand-mixed blends in both DE and porosity. Furthermore, the 2080-C and 3070-C deposits also demonstrated the best retention of composition, exhibiting almost no loss of Cu after cold spray. By analyzing the cryomilled feedstocks as well as the surfaces and cross sections of the deposits via SEM, we conclude that this is due to both the combination and length scale of deposition mechanisms and material interactions at play in the cryomilled blends. In the feedstock powders with high volume fractions of PEEK, Cu primarily appeared in micron-scale domains coating the outer surface of PEEK particles and in dense, consolidated particles compared to the dendritic Cu masses found in the hand-mixed powders. This combination, along with the reduced volume fraction of Cu, shifted the dominant mechanisms of deposition to encourage both embedding and deformation of solid Cu particles without rebounding or inducing porosity. Particles that did still rebound likely exhibited a peening effect, allowing PEEK domains to further deform and fill in any porosity that still occurred. Hand-mixed blends, conversely, showed much less Cu embedding on deposit surfaces, indicating that particle rebounding was much more likely. The lower Cu fractions measured by TGA after deposition agree with this theory. Further, increased porosity and visible particle boundaries within the same deposits indicated less favorable interactions between the impacting particles of hand-mixed blends compared to cryomilled composite powders.

The ability to successfully cold spray and deposit Cu-PEEK composite powders allows for bond layers to be created on PEEK-matrix composites to metallize polymer

rich substrates and structures, which may allow for the production of stronger, thicker, and more well-adhered metallic coatings. In the future, producing a functionally graded cold-sprayed deposit of increasing Cu content to neat Cu would show the ability to create a continuous Cu network. Since the cryomilling technique to create composite powders detailed in this paper is only dependent on the relative hardness of the starting materials, it can be applied to other metal–polymer combinations for a broad range of applications in various high-performance material industries.

The authors acknowledge that cryomilling may introduce work hardening to the Cu particles that disproportionally affect deposits of higher Cu fractions. In the C powders of lower Cu fraction, work hardening in the Cu particles would increase the likelihood of embedding in the PEEK substrate and inducing greater deformation of the polymer. This could also serve as an alternative explanation for the improved composition retention in the cryomilled blends, as rebounding would be less likely to occur. However, at higher compositions, the effects of work hardening cannot be isolated from those of the mild cold spray conditions on an increasingly Cu-rich composite powder. Since the primary mechanism of Cu deposition observed in this study is by embedding in PEEK, it becomes increasingly difficult to discern whether rebounding of Cu particles is due to work hardening inhibiting deformation or simply by the fact that Cu does not undergo like-on-like deposition under the conditions studied.

Acknowledgements This research was supported by Army Research Laboratory contract W911NF-19-2-0152. The views and conclusions contained in this document are those of the authors and should not be interpreted as representing the official policies, either expressed or implied, of the U.S. Army Research Laboratory or the U.S. Government. The U.S. Government is authorized to reproduce and distribute reprints for Government purposes notwithstanding any copyright notation herein.

Funding Open access funding provided by Rowan University.

References

1. R. Della Gatta, A.S. Perna, and A. Viscusi, Cold Spray Deposition of Metallic Coatings on Polymers: A Review, *J. Mater. Sci.*, 2021, **57**(1), p 27-57.
2. V. Gillet, E. Aubignat, S. Costil, B. Courant, C. Langlade, P. Casari, and W. Knapp, Development of Low Pressure Cold Sprayed Copper Coatings on Carbon Fiber Reinforced Polymer (CFRP), *Surf. Coat. Technol.*, 2019, **364**, p 306-316.
3. P.S.M. Rajesh, F. Sirois, and D. Therriault, Damage Response of Composites Coated with Conducting Materials Subjected to Emulated Lightning Strikes, *Mater. Des.*, 2018, **139**, p 45-55.
4. V. Bortolussi, B. Figliuzzi, F. Willot, M. Faessel, and M. Jeandin, Electrical Conductivity of Metal-Polymer Cold Spray Composite Coatings onto Carbon Fiber-Reinforced Polymer, *J. Therm. Spray Technol.*, 2020, **29**(4), p 642-656.
5. P. Lomonaco, S. Weiller, I. Feki, A. Debray, F. Delloro, M. Jeandin, B. Favini, and C. Rossignol, Cold Spray Technology to Promote Conductivity of Short Carbon Fiber Reinforced Polyether-Ether-Ketone (PEEK), *Key Eng. Mater.*, 2019, **813**, p 459-464.
6. C. Chen, X. Xie, Y. Xie, X. Yan, C. Huang, S. Deng, Z. Ren, and H. Liao, Metallization of polyether ether ketone (PEEK) by copper coating via cold spray, *Surf. Coat. Technol.*, 2018, **342**(1), p 209-219.
7. G. Bae, Y. Xiong, S. Kumar, K. Kang, and C. Lee, General Aspects of Interface Bonding in Kinetic Sprayed Coatings, *Acta Mater.*, 2008, **56**, p 4858-4868.
8. M. Tului et al., in Copper-based Alloy Reinforced with Hard Particle and Deposited via Cold Gas Spray, ASM International, (Wien, Wien, Austria, 2022)
9. R. Serra-Gomez, G. Gonzalez-Gaitano, and J. Gonzalez-Benito, Composites Based on EVA and Barium Titanate Submicrometeric Particles: Preparation by High-Energy Ball Milling and Characterization, *Polym. Compos.*, 2012, **33**(9), p 1549-1556.
10. Z. Khalkhali et al., A Comparison of Cold Spray Technique to Single Particle Micro-ballistic Impacts for the Deposition of Polymer Particles on Polymer Substrates, *Surf. Coat. Technol.*, 2018, **351**, p 99-107.
11. M.S. Kaminskyj, M.S. Schwenger, D.A. Brennan, F.M. Haas, and J.F. Stanzione III, in Effects of Polymer Crystallinity on Deposition Efficiency and Porosity in Cold Spray of PEKK, ASM International, (Wien, Wien, Austria, 2022), p 82-88
12. T.W. Bacha, E.M. Henning, L. Elwell, F.M. Haas, and J.F. Stanzione III, in Cold Spray Additive Manufacturing of Polymers: Temperature Profiles Dictate Properties Upon Deposition, *SAMPE North America* TP20-0000000140, 2020
13. T.W. Bacha, D.A. Brennan, U. Tiitma, I.M. Nault, F.M. Haas, and J.F. Stanzione III., Effects of Powder Feedstock Pre-Heating on Polymer Cold Spray Deposition, *J. Therm. Spray Tech.*, 2023, **32**, p 488-501.
14. M.S. Schwenger, M.S. Kaminskyj, F.M. Haas, and J.F. Stanzione III, in Mixed-Material Feedstocks for Cold Spray Additive Manufacturing of Metal-Polymer Composites, ASM International, (Quebec City, Quebec, Canada, 2023), p 186-191